

Role of Curvature-Matter Coupling on Anisotropic Strange Stars

M. Sharif *and Arfa Waseem †

Department of Mathematics, University of the Punjab,
Quaid-e-Azam Campus, Lahore-54590, Pakistan.

Abstract

In this paper, we study the physical characteristics of anisotropic spherically symmetric quark star candidates for $R+2\sigma T$ gravity model, where R , σ and T depict scalar curvature, coupling parameter, and the trace of the energy-momentum tensor, respectively. In order to analyze the structure formation of quark stars, we consider the Heintzmann solution and assume that strange quark matter is characterized by MIT bag model equation of state. We evaluate the unknown parameters through matching conditions and obtain the values of radii of strange quark stars using modified Tolman-Oppenheimer-Volkoff equation with observed values of masses and bag constant. The feasibility of our considered solution is analyzed by graphical analysis of matter variables, energy bounds, causality condition and adiabatic index. It is found that the strange quark stars show stable structure corresponding to Heintzmann solution and their physical viability enhances with increasing values of the model parameter σ .

Keywords: Quark stars; Anisotropy; $f(R, T)$ gravity; MIT bag model.

PACS: 04.50.Kd; 97.60.Jd.

*msharif.math@pu.edu.pk

†arfawaseem.pu@gmail.com

1 Introduction

The revolutionary developments in modern cosmology as well as astrophysics provide a new inspiration about the universe and its mysterious constituents. Despite the marvelous discoveries, there are still various challenging problems which stimulate the researchers to explore the hidden mysteries of these constituents such as stars, galaxies and their respective physical phenomena. Stars are mostly recognized as the basic ingredients of galaxy and identified as the fundamental constituent in astronomy. The nuclear fusion reactions in the core of a star exhibit a dynamical behavior in the structure constitution as well as evolution of astrophysical objects. The fusion processes in the star core generate outward directed thermal pressure to overcome the gravitational pull produced by a star mass. Once the nuclear fuel is entirely burnt out, there remains no sufficient pressure to resist the attractive force of gravity, consequently, the star experiences the stellar death, a phenomenon known as gravitational collapse.

This collapse is responsible for the existence of massive stars referred to as compact objects which are classified as white dwarfs, neutron stars and black holes based on the masses of parent stars. The study of interior configuration of compact stars has inspired many observers to inspect their diverse features. In compact objects, neutron stars have gained much attention due to their compelling properties and structure compositions. In neutron stars, the degeneracy pressure produced by the neutrons counterbalances the gravitational pull to keep the star in a hydrostatic equilibrium state. The structure of neutron stars with less dense core provides an opportunity to transform into quark stars. The densest compact objects composed of up, down and strange quark matter are named as quark stars. This hypothetical compact object has drawn the attention of many researchers to explore its interior formation [1]-[10].

In the analysis of structural properties of compact objects, anisotropic matter configuration plays a crucial role. Since the compact objects possess dense cores and have densities much larger than the nuclear density, therefore, pressure should be anisotropic in the interior region of celestial bodies [11]. It is anticipated that the interior constitution of quark stars is expressed by MIT bag model equation of state (EoS) [3, 10]. Many people examined the features of compact objects characterized by this EoS along with anisotropic matter configuration. Demorest et al. [12] evaluated the mass of strange quark star (PSR J1614-2230) and determined that such massive compact objects can

only be supported by MIT bag model EoS. Kalam et al. [13] considered a specific ansatz on the radial metric function to examine the features of strange star candidates (SAX J 1808.4-3658, Her X-1 and 4U 1820-30) for this EoS. They obtained non-singular solutions of the field equations and found that their solutions satisfy all the regularity conditions.

Rahaman et al. [14] analyzed the presence of strange quark stars using an interpolation function for mass and observed the physical characteristics of stars associated with MIT bag model EoS. For anisotropic distribution, Bhar [15] established a new hybrid star model by considering Krori-Barua ansatz with the same EoS. She found that all the physical constraints are fulfilled and the value of mass function is very close to the observational data. Murad [16] investigated the effects of charge on the composition as well as nature of anisotropic quark stars. Arbañil and Malheiro [17] discussed the impact of anisotropic factor on the stability of compact stars via numerical solution of radial perturbation, the hydrostatic equilibrium and MIT bag model. Deb and his collaborators [18] obtained non-singular anisotropic solutions for quark stars using the same EoS and presented the graphical behavior of matter variables as well as energy constraints for LMC X-4 star model.

General relativity (GR) has made remarkable achievements in resolving various hidden puzzles of the cosmos but it is not adequate to inspect the universe at large scales. In this regard, alternative theories to GR are identified as the most effective approaches to deal with the stimulating mysteries such as dark matter and current accelerated cosmic expansion. This expansion ensures the appearance of an enigmatic force with large negative pressure dubbed as dark energy. Modified or extended theories of gravity have shown a fundamental role to explore the diverse features of dark energy and dark matter.

The simplest extension to GR is $f(R)$ theory [19] originated by placing a generic function $f(R)$ instead of curvature scalar (R) in the Einstein-Hilbert action. Other modified theories such as $f(\mathcal{G})$ gravity (\mathcal{G} shows Gauss-Bonnet scalar) [20] and $f(\mathcal{T})$ gravity (\mathcal{T} stands for torsion scalar) [21] have achieved much attention due to joined inspiration arising from cosmology, high-energy physics and astrophysics. The fascinating feature of extended theories is based on the coupling between matter and gravitational fields. Such type of coupling provides an extra force which may yield interesting results and helps to inspect hidden puzzles causing the cosmic expansion. This leads to various modified theories having strong curvature-matter coupling like $f(R, T)$ theory [22], $f(R, T, R_{\gamma\delta}T^{\gamma\delta})$ theory [23] and $f(\mathcal{G}, T)$ gravity [24].

The $f(R, T)$ theory as an extended form of $f(R)$ gravity has inspired many researchers and is employed to narrate distinct cosmological [25]-[34] and astrophysical [35]-[43] scenarios. This theory has provided many fascinating results in the evolution of compact objects associated with MIT bag model EoS as well as anisotropic matter configuration. In this context, Sharif and Siddiqua [44] examined the influence of curvature-matter coupling on the structure formation of compact stars by using the MIT bag model and polytropic EoS for some specific choices of the coupling parameters. Deb et al. [45] derived the analytic solutions for anisotropic strange stars with same EoS and discussed the physical behavior of LMC X-4 as an example of quark star. The influence of electric field on the stability of Her X-1, 4U1820-30 and SAX J 1808.4- 3658 star candidates are also investigated in this gravity [46]. Biswas et al. [47] analyzed the anisotropic quark star models using Krori-Barua solution with bag constant and observed the graphical behavior of various physical quantities for three particular stars.

Recently, Deb et al. [48] examined the properties of 12 strange quark star candidates by assuming MIT bag model EoS for $R+2\sigma T$ gravity model. They obtained the values of central energy density and pressure for considered star models by employing Lake solution and presented the graphical analysis for LMC X-4 star candidate. For the same model, Maurya et al. [49] analyzed the behavior of strange stars by adopting the embedding class one technique. In this paper, we study the influence of anisotropic factor and MIT bag model EoS on different strange star models by considering the Heintzmann solution for $R + 2\sigma T$ gravity model. The paper is organized as follows. Next section deals with the formulation of anisotropic $f(R, T)$ field equations corresponding to Heintzmann ansatz. In section **3**, we derive the values of Heintzmann constants by using boundary conditions at the surface of star. Section **4** exhibits the graphical interpretation of physical analysis of considered strange star models. Final remarks are given in the last section.

2 The $f(R, T)$ Field Equations

The action of $f(R, T)$ theory associated with matter Lagrangian (\mathcal{L}_m) is specified by [22]

$$\mathcal{I}_{f(R,T)} = \int \left[\frac{f(R, T)}{2\kappa} + \mathcal{L}_m \right] \sqrt{-g} d^4x, \quad (1)$$

in which $\kappa = 1$ stands for coupling constant and g reveals the determinant of the metric tensor ($g_{\gamma\delta}$). The corresponding $f(R, T)$ field equations are

$$\begin{aligned} f_R(R, T)R_{\gamma\delta} &- (\nabla_\gamma\nabla_\delta - g_{\gamma\delta}\square)f_R(R, T) - \frac{1}{2}g_{\gamma\delta}f(R, T) \\ &= T_{\gamma\delta} - (\Theta_{\gamma\delta} + T_{\gamma\delta})f_T(R, T), \end{aligned} \quad (2)$$

where $f_R(R, T) = \frac{\partial f(R, T)}{\partial R}$, $f_T(R, T) = \frac{\partial f(R, T)}{\partial T}$, $\square = g^{\gamma\delta}\nabla_\gamma\nabla_\delta$, ∇_γ is the covariant derivative and $\Theta_{\gamma\delta}$ is characterized by

$$\Theta_{\gamma\delta} = g^{\mu\nu}\frac{\delta T_{\mu\nu}}{\delta g^{\gamma\delta}} = g_{\gamma\delta}\mathcal{L}_m - 2T_{\gamma\delta} - 2g^{\mu\nu}\frac{\partial^2\mathcal{L}_m}{\partial g^{\gamma\delta}\partial g^{\mu\nu}}. \quad (3)$$

The covariant divergence of Eq.(2) provides

$$\nabla^\gamma T_{\gamma\delta} = \frac{f_T}{1 - f_T} \left[(T_{\gamma\delta} + \Theta_{\gamma\delta})\nabla^\gamma(\ln f_T) - \frac{g_{\gamma\delta}}{2}\nabla^\gamma T + \nabla^\gamma\Theta_{\gamma\delta} \right]. \quad (4)$$

This equation demonstrates that the energy-momentum tensor (EMT) does not satisfy the conservation equation similar to other modified theories [22].

In astrophysics, the matter configuration is characterized by EMT in which all non-vanishing components express dynamical quantities associated with some physical impacts. In the analysis of strange compact structures, the anisotropy produced by pressure is considered as a crucial ingredient which influences their structure development. As the stellar distribution is mostly found to be rotating as well as anisotropic therefore, the anisotropic parameter has persuasive effects in different dynamical phases of stellar transformation. The effect of anisotropy appears from the difference of radial and transverse pressure components. Here, we discuss the physical features of strange quark stars under the influence of pressure anisotropy. We consider that the internal matter distribution of stellar models is comprised by anisotropic matter configuration whose mathematical description is

$$T_{\gamma\delta} = (\rho + p_t)U_\gamma U_\delta - p_t g_{\gamma\delta} + (p_r - p_t)X_\gamma X_\delta, \quad (5)$$

where ρ indicates matter energy density, p_t and p_r are transverse and radial pressure entities, respectively, U_γ acts as four velocity and X_γ denotes the four-vector. The four velocity and four-vector in comoving coordinates satisfy

$$U^\gamma U_\gamma = 1, \quad X_\gamma X^\gamma = -1.$$

In the distribution of matter, there are various choices of \mathcal{L}_m . Here, we assume $\mathcal{L}_m = -\mathcal{P}$, where $\mathcal{P} = \frac{p_r + 2p_t}{3}$ leading to $\frac{\partial^2 \mathcal{L}_m}{\partial g^{\gamma\delta} \partial g^{\mu\nu}} = 0$ [22] and hence, $\Theta_{\gamma\delta} = -2T_{\gamma\delta} - \mathcal{P}g_{\gamma\delta}$. This form of matter Lagrangian has been used in literature [47]-[49] to analyze the nature of compact objects.

To analyze the coupling outcomes of curvature and matter ingredients in $f(R, T)$ scenario on the strange quark candidates, we choose an independent model given as

$$f(R, T) = f_1(R) + f_2(T). \quad (6)$$

The $f(R, T)$ gravity includes T that narrates more modified forms of GR in comparison with $f(R)$ gravity. It is obvious that a compatible as well as feasible model reveals the choices for coupling constants whose values lie in the observational limits. We consider $f_1(R) = R$ and $f_2(T) = 2\sigma T$, where $T = \rho - p_r - 2p_t$. This particular model is firstly suggested by Harko et al. [22] and has been used extensively to study the features of astrophysical objects [50, 51]. Recently, Deb et al. [48] found analytic solution of the generalized form of Tolman-Oppenheimer-Volkoff (TOV) equation for this model and discussed the features of various physical parameters for different values of σ . Sharif and Siddiqa [52] examined the expanding as well as collapsing solutions corresponding to charged cylindrical system and observed the viability of their solutions in the same functional form.

On inserting the specific model along with the considered choice of \mathcal{L}_m in Eq.(2), we obtain

$$G_{\gamma\delta} = T_{\gamma\delta} + \sigma T g_{\gamma\delta} + 2\sigma(T_{\gamma\delta} + \mathcal{P}g_{\gamma\delta}) = T_{\gamma\delta}^{eff}, \quad (7)$$

where $G_{\gamma\delta}$ shows the standard Einstein tensor and $T_{\gamma\delta}^{eff}$ represents effective EMT. For $\sigma = 0$, the standard results of GR can be retrieved from Eq.(7). The covariant divergence (4) corresponding to $R + 2\sigma T$ model becomes

$$\nabla^\gamma T_{\gamma\delta} = \frac{-\sigma}{1 + 2\sigma} [g_{\gamma\delta} \nabla^\gamma T + 2\nabla^\gamma (\mathcal{P}g_{\gamma\delta})]. \quad (8)$$

In order to characterize the internal geometry of quark stars, we take the static spherical stellar distribution expressed by the metric

$$ds_-^2 = e^{\chi(r)} dt^2 - e^{\eta(r)} dr^2 - r^2 d\theta^2 - r^2 \sin^2 \theta d\phi^2. \quad (9)$$

Equations (5), (7) and (9) lead to the following field equations

$$\frac{1}{r^2} - e^{-\eta} \left(\frac{1}{r^2} - \frac{\eta'}{r} \right) = \rho + \frac{\sigma}{3} (9\rho - p_r - 2p_t) = \rho^{eff}, \quad (10)$$

$$e^{-\eta} \left(\frac{1}{r^2} + \frac{\chi'}{r} \right) - \frac{1}{r^2} = p_r - \frac{\sigma}{3}(3\rho - 7p_r - 2p_t) = p_r^{eff}, \quad (11)$$

$$e^{-\eta} \left(\frac{\chi''}{2} - \frac{\eta'}{2r} + \frac{\chi'}{2r} + \frac{\chi'^2}{4} - \frac{\chi'\eta'}{4} \right) = p_t - \frac{\sigma}{3}(3\rho - p_r - 8p_t) = p_t^{eff}. \quad (12)$$

Here prime reveals differentiation corresponding to r and matter variables ρ^{eff} , p_r^{eff} and p_t^{eff} indicate the effective energy density, effective radial pressure and effective transverse pressure of the compact system, respectively.

In order to solve the system (10)-(12), we suppose that inside the stellar models, physical quantities of the fluid distribution are related through the MIT bag model EoS. This EoS plays a dynamical role for the relativistic modeling of quark stars [3, 10]. For massless as well as non-interacting strange quarks matter in the bag model, the radial pressure is

$$p_r = \sum_{q=u,d,s} p^q - \mathfrak{B}, \quad (13)$$

with p^q stands for the individual pressure corresponding to each quark matter (up (u), down (d) and strange (s)) and \mathfrak{B} denotes the bag constant. The matter density with respect to individual quark flavor is associated with the pressure as $\rho^q = 3p^q$. Consequently, the energy density for free quarks in the bag model becomes

$$\rho = \sum_{q=u,d,s} \rho^q + \mathfrak{B}. \quad (14)$$

Using Eqs.(13) and (14), the EoS for MIT bag model describing the strange matter of quarks is derived as follows

$$p_r = \frac{1}{3}(\rho - 4\mathfrak{B}). \quad (15)$$

To inspect the physical characteristics of quark star candidates, many researchers have successfully used the MIT bag model EoS with different choices of bag constant [13]-[18]. The study of static spherically stellar system requires the following definition of mass function

$$m(r) = 4\pi \int_0^r r^2 \rho^{eff} dr. \quad (16)$$

Insertion of Eq.(16) into (10) leads to

$$e^{-\eta(r)} = 1 - \frac{2m(r)}{r}, \quad (17)$$

where m represents the interior mass of a spherical object.

2.1 Heintzmann Solution

To examine the features of strange quark stars, we consider a particular form of metric potentials proposed by Heintzmann [53] and defined as

$$e^{\chi(r)} = \mathcal{A}^2(1 + ar^2)^3, \quad e^{\eta(r)} = \left[1 - \frac{3ar^2}{2} \left\{ \frac{1 + c(1 + 4ar^2)^{\frac{-1}{2}}}{1 + ar^2} \right\} \right]^{-1}, \quad (18)$$

where \mathcal{A} , a and c are unknown constants. Heintzmann provided this solution as the new Einstein static solution which may generate interesting results in astrophysics. This solution is also named as Heint IIa solution. Recently, Estrada and Tello-Ortiz [54] used this solution as an interior solution to obtain the new anisotropic solution via gravitational decoupling approach. They also analyzed the behavior of matter variables and stability criterion for particular compact star models. Morales and Tello-Ortiz [55] also formulated charged anisotropic solutions of the Einstein field equations by extending the Heintzmann solution through gravitational decoupling technique.

Substituting Eq.(18) in (10)-(12) and using (15), we obtain

$$\rho^{eff} = \frac{-9a \left[(-3 + ar^2)(1 + 4ar^2)^{\frac{3}{2}} + c(-1 + ar^2 + 14a^2r^4) \right]}{4(1 + 2\sigma)(1 + ar^2)^2(1 + 4ar^2)^{\frac{3}{2}}} + \mathfrak{B}, \quad (19)$$

$$p_r^{eff} = \frac{3a \left[(3 - ar^2)(1 + 4ar^2)^{\frac{3}{2}} + c(1 - ar^2 - 14a^2r^4) \right]}{4(1 + 2\sigma)(1 + ar^2)^2(1 + 4ar^2)^{\frac{3}{2}}} - \mathfrak{B}, \quad (20)$$

$$\begin{aligned} p_t^{eff} &= \frac{1}{2(1 + 2\sigma)(3 + 8\sigma)(1 + ar^2)^2(1 + 4ar^2)^{\frac{3}{2}}} \left[8\sigma(1 + 2\sigma)\sqrt{1 + 4ar^2}\mathfrak{B} \right. \\ &+ 4a^3r^4 \left\{ \sqrt{1 + 4ar^2}(2\sigma(-33 + 4\mathfrak{B}r^2(1 + 2\sigma)) - 27) - 21c(3 + 8\sigma) \right\} \\ &+ 3a \left\{ \sqrt{1 + 4ar^2}(9 + 2\sigma(15 + \mathfrak{B}r^2(1 + 2\sigma))) - c(3 + 2\sigma) \right\} + 3a^2r^2 \\ &\times \left. \left\{ \sqrt{1 + 4ar^2}(27 + 2\sigma(49 + 12\mathfrak{B}r^2(1 + 2\sigma))) - c(33 + 70\sigma) \right\} \right]. \quad (21) \end{aligned}$$

For $\sigma = 0$, these reduce to GR equations corresponding to MIT bag model EoS. The mathematical form of anisotropic factor can be evaluated as

$$\begin{aligned} \Delta^{eff} = p_t^{eff} - p_r^{eff} = & \frac{3}{4(1+2\sigma)(3+8\sigma)(1+ar^2)^2(1+4ar^2)^{\frac{3}{2}}} \left[4(1+6\sigma \right. \\ & + 8\sigma^2)\sqrt{1+4ar^2}\mathfrak{B} + 3a\left\{ \sqrt{1+4ar^2}(1+4\sigma)(3+8\mathfrak{B}r^2(1+2\sigma)) \right. \\ & - c(3+4\sigma) \left. \right\} + 3a^2r^2\left\{ \sqrt{1+4ar^2}(7+36\sigma+12\mathfrak{B}r^2(1+6\sigma+8\sigma^2)) \right. \\ & - c(21+44\sigma) \left. \right\} + 2a^3r^4\left\{ 2\sqrt{1+4ar^2}(-3(5+12\sigma)+4\mathfrak{B}r^2(1+6\sigma \right. \\ & \left. + 8\sigma^2)) \right\} \left. \right]. \end{aligned} \quad (22)$$

3 Boundary Conditions

To examine the nature as well as physical features of anisotropic strange quark stars, there must exist a smooth relationship between both (interior and exterior) regions of compact objects. In this regard, we choose the Schwarzschild metric presented by

$$ds_+^2 = \left(1 - \frac{2\mathcal{M}}{r}\right) dt^2 - \left(1 - \frac{2\mathcal{M}}{r}\right)^{-1} dr^2 - r^2 d\theta^2 - r^2 \sin^2 \theta d\phi^2, \quad (23)$$

where \mathcal{M} acts as total mass within the boundary ($r = \mathcal{R}$) of stellar model. At $r = \mathcal{R}$, the continuity of metric coefficients g_{tt} , g_{rr} and $g_{tt,r}$ leads to

$$1 - \frac{2\mathcal{M}}{\mathcal{R}} = \mathcal{A}^2(1+a\mathcal{R}^2)^3, \quad (24)$$

$$\left(1 - \frac{2\mathcal{M}}{\mathcal{R}}\right)^{-1} = \left[1 - \frac{3a\mathcal{R}^2}{2} \left\{ \frac{1+c(1+4a\mathcal{R}^2)^{-1/2}}{1+a\mathcal{R}^2} \right\}\right]^{-1}, \quad (25)$$

$$\frac{\mathcal{M}}{\mathcal{R}^2} = 3a\mathcal{A}^2\mathcal{R}(1+a\mathcal{R}^2)^2. \quad (26)$$

The unknown triplet (\mathcal{A}, a, c) corresponding to radius and total mass can be obtained from Eqs.(24)-(26) which provide

$$\mathcal{A} = \sqrt{\frac{(\mathcal{R}-2\mathcal{M})(3\mathcal{R}-7\mathcal{M})^3}{\mathcal{R}(3\mathcal{R}-6\mathcal{M})^3}}, \quad (27)$$

$$a = \frac{\mathcal{M}}{\mathcal{R}^2(3\mathcal{R} - 7\mathcal{M})}, \quad (28)$$

$$c = \left(\frac{3\mathcal{R} - 8\mathcal{M}}{\mathcal{R}} \right) \sqrt{\frac{3(\mathcal{R} - \mathcal{M})}{3\mathcal{R} - 7\mathcal{M}}}. \quad (29)$$

In $f(R, T)$ scenario, the modified form of generalized TOV equation is

$$-p'_r - \frac{\chi'}{2}(\rho + p_r) + \frac{2}{r}(p_t - p_r) + \frac{\sigma}{3(1+2\sigma)}(3\rho' - p'_r - 2p'_t) = 0. \quad (30)$$

This equation along with Eqs.(11) and (17) provide the hydrostatic equilibrium equation for anisotropic compact object in $f(R, T)$ background as

$$p'_r = \frac{-\left[(\rho + p_r) \left\{ \frac{r^2}{2} p_r + \frac{m}{r} - \frac{\sigma}{6}(3\rho - 7p_r - 2p_t) \right\}\right] + 2(p_t - p_r) \left(1 - \frac{2m}{r}\right)}{r \left(1 - \frac{2m}{r}\right) \left\{ 1 + \frac{\sigma}{3(1+2\sigma)} \left(1 - \frac{3\rho'}{p'_r} + \frac{2p'_t}{p'_r}\right) \right\}}. \quad (31)$$

This equation reduces to the standard hydrostatic equation in GR for $\sigma = 0$. Using condition $p_r(\mathcal{R}) = 0$ and Eqs.(27)-(29) in Eq.(20), we obtain total mass of the strange star as

$$\mathcal{M} = \frac{\mathcal{R}}{28} \left[9 + 6\mathfrak{B}\mathcal{R}^2(1+2\sigma) - \sqrt{\{9 + 6\mathfrak{B}\mathcal{R}^2(1+2\sigma)\}^2 - 336(1+2\sigma)\mathfrak{B}\mathcal{R}^2} \right]. \quad (32)$$

To evaluate the values of radii of the strange quark star models, we solve Eq.(31) using expressions given in (15), (19) and (21) for the observed values of masses of some particular star candidates [12], [56]-[61] with $\sigma = 0.8$ and $\mathfrak{B} = 64 \text{ MeV}/\text{fm}^3$. Table 1 gives the values of predicted radii, compactness parameter and surface gravitational redshift with respect to the masses of some strange star candidates. It is interesting to mention here that the values of these parameters are close to the values obtained by considering different forms of metric functions in $f(R, T)$ framework for $\mathfrak{B} = 83 \text{ MeV}/\text{fm}^3$ [48] and $\mathfrak{B} = 64 \text{ MeV}/\text{fm}^3$ [49]. Using the values of masses and predicted radii of proposed strange stars, we evaluate the values of Heintzmann constants (\mathcal{A}, a, c) given in Table 2.

4 Physical Features of Strange Quark Stars

Here we analyze the physical properties of proposed anisotropic star models. Using the calculated values of radii and Heintzmann constants given in

Table 1: Physical values of the stellar models for $\mathfrak{B} = 64\text{MeV}/fm^3$ and $\sigma = 0.8$.

Star Models	Mass (M_{\odot})	Predicted Radius (km)	$\frac{M}{R}$	z_s
Her X-1	0.85 ± 0.15	7.64 ± 0.20	0.163	0.218
SAX J1808.4-3658	0.9 ± 0.3	8.05 ± 0.71	0.164	0.219
SMC X-1	1.04 ± 0.09	9.25 ± 0.24	0.165	0.222
LMC X-4	1.29 ± 0.05	10.58 ± 0.11	0.178	0.246
EXO 1785-248	1.3 ± 0.2	10.68 ± 0.46	0.179	0.248
Cen X-3	1.49 ± 0.08	11.06 ± 0.31	0.198	0.287
4U 1820-30	1.58 ± 0.06	11.70 ± 0.12	0.199	0.289
PSR J 1903+0327	1.667 ± 0.021	11.82 ± 0.05	0.207	0.306
Vela X-1	1.77 ± 0.08	12.08 ± 0.10	0.215	0.324
PSR J 1614-2230	1.97 ± 0.04	12.76 ± 0.03	0.227	0.353

Table 2: Calculated values of Heintzmann constants for different star models.

Star Models	\mathcal{A}	a	c
Her X-1	0.722669	15.2×10^{-4}	1.9674
SAX J1808.4-3658	0.721113	14.3×10^{-4}	1.96198
SMC X-1	0.719306	10.5×10^{-4}	1.95569
LMC X-4	0.691716	9.2×10^{-4}	1.86018
EXO 1785-248	0.692321	9.0×10^{-4}	1.86226
Cen X-3	0.653257	10.0×10^{-4}	1.72859
4U 1820-30	0.652265	9.0×10^{-4}	1.72522
PSR J 1903-327	0.633688	9.6×10^{-4}	1.66224
Vela X-1	0.616326	9.9×10^{-4}	1.60367
PSR J 1614-2230	0.590875	9.8×10^{-4}	1.51825

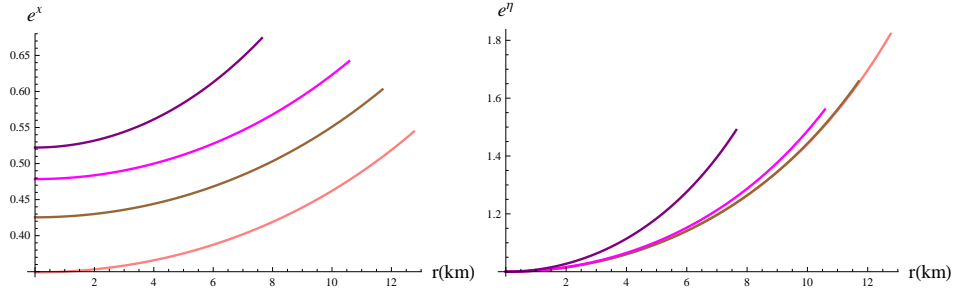


Figure 1: Behavior of metric potentials versus r for Her X-1 (purple), LMC X-4 (magenta), 4U 1820-30 (brown) and PSR J 1614-2230 (pink).

Tables **1** and **2**, respectively, we study the behavior of various physical parameters. We examine the viability of metric potentials and investigate the effective energy density, effective radial and transverse pressure components, anisotropic parameter, mass-radius relation, energy conditions and stability for different values of the coupling parameter. It is well-known that for a physically consistent solution, the metric coefficients must be singularity free, monotonically increasing and positive functions of r . The metric coefficients depend only on Heintzmann constants as shown in Eq.(18). Using the values of these constants from Table **2** for some particular star models, the behavior of metric functions is exhibited in Figure **1** which shows that the metric functions are viable with all the respective conditions and are physically consistent.

4.1 Analysis of Matter Components

In the analysis of compact stellar objects, it is required that the realistic compact structures should possess maximum pressure and energy density in the core of a star. For different choices of σ , the variation of effective energy density, effective pressure (transverse/radial) and anisotropic component inside the LMC X-4 star model is shown in Figure **2**. In these Figures, $\sigma = 0$ represents the standard GR results obtained in terms of Heintzmann constants for $\mathfrak{B} = 64 \text{MeV}/\text{fm}^3$. We analyze the graphical behavior of all the proposed star models but here we show the graphical analysis only for LMC X-4 star model. Figure **2** indicates that the effective energy density and effective pressure components depict extreme values at the center of star. These values show monotonically decreasing behavior towards the boundary

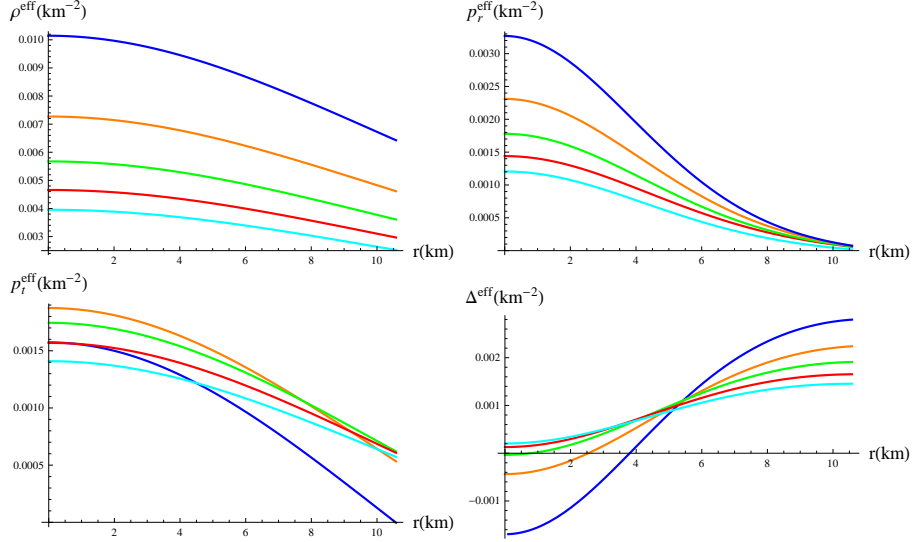


Figure 2: Variation of matter variables versus r for LMC X-4 with $\sigma = 0$ (blue), $\sigma = 0.2$ (orange), $\sigma = 0.4$ (green), $\sigma = 0.6$ (red) and $\sigma = 0.8$ (cyan).

surface which confirm the presence of highly dense as well as compact cores.

It is also observed that the value of radial pressure approximately equals to zero at $r = \mathcal{R}$ for small values of σ and completely vanishes at $\sigma = 0.8$. Moreover, the behavior of anisotropic factor shows the variation from negative to positive values with increasing values of σ . We can conclude that the Heintzmann solution expresses the more viable behavior of anisotropic factor and vanishing condition of radial pressure for $\sigma = 0.8$. Table **3** provides the values of effective central energy density (ρ_c^{eff}), effective energy density at the boundary surface (ρ_0^{eff}) and effective central radial pressure (p_{rc}^{eff}) corresponding to $\sigma = 0.8$ and $\mathfrak{B} = 64 \text{MeV}/\text{fm}^3$ for all considered strange star models. We note that these values of energy density and pressure are larger than the values obtained for Lake solution in $f(R, T)$ scenario for $\sigma = -0.4$ and $\mathfrak{B} = 83 \text{MeV}/\text{fm}^3$ [48].

In Figure **3**, we present the behavior of total mass normalized in units of solar mass with respect to the total radius of the strange star candidates for different values of σ and the specific chosen value of bag constant. It is found that the mass increases with increasing value of model parameter and the maximum mass is $0.2M_\odot$ when $\sigma = 0.8$. Hence, we conclude that

Table 3: Observed values of ρ_c^{eff} , ρ_0^{eff} and p_{rc}^{eff} for $\sigma = 0.8$ and $\mathfrak{B} = 64MeV/fm^3$.

Star Models	$\rho_c^{eff}(gm/cm^3)$	$\rho_0^{eff}(gm/cm^3)$	$p_{rc}^{eff}(dyne/cm^2)$
Her X-1	8.98×10^{15}	5.98×10^{15}	2.8×10^{36}
SAX J1808.4-3658	8.3×10^{15}	5.4×10^{15}	2.6×10^{36}
SMC X-1	6.3×10^{15}	4.1×10^{15}	1.9×10^{36}
LMC X-4	5.4×10^{15}	3.5×10^{15}	1.6×10^{36}
EXO 1785-248	5.3×10^{15}	3.4×10^{15}	1.6×10^{36}
Cen X-3	5.8×10^{15}	3.6×10^{15}	1.6×10^{36}
4U 1820-30	5.1×10^{15}	3.0×10^{15}	1.4×10^{36}
PSR J 1903-327	5.3×10^{15}	3.4×10^{15}	1.5×10^{36}
Vela X-1	5.5×10^{15}	3.1×10^{15}	1.6×10^{36}
PSR J 1614-2230	5.3×10^{15}	2.9×10^{15}	1.5×10^{36}

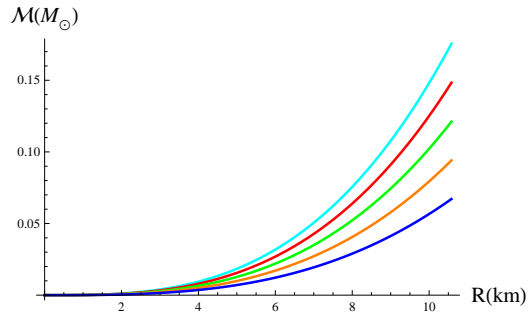


Figure 3: Variation of total mass versus total radius for LMC X-4 with $\sigma = 0$ (blue), $\sigma = 0.2$ (orange), $\sigma = 0.4$ (green), $\sigma = 0.6$ (red) and $\sigma = 0.8$ (cyan).

the increasing values of σ lead to the more massive and less dense compact objects.

4.2 Energy Bounds

The energy bounds have significant importance in illustrating the existence of matter distribution. These bounds are utilized to characterize the ordinary or exotic configuration of matter inside the stellar objects as well as to examine the viability of the theory. In $f(R, T)$ gravity for anisotropic fluid distribution, these bounds are classified as [62]

- Null : $\rho^{eff} + p_r^{eff} \geq 0, \quad \rho^{eff} + p_t^{eff} \geq 0,$
- Weak: $\rho^{eff} \geq 0, \quad \rho^{eff} + p_r^{eff} \geq 0, \quad \rho^{eff} + p_t^{eff} \geq 0,$
- Strong: $\rho^{eff} + p_r^{eff} \geq 0, \quad \rho^{eff} + p_t^{eff} \geq 0, \quad \rho^{eff} + p_r^{eff} + 2p_t^{eff} \geq 0,$
- Dominant: $\rho^{eff} - p_r^{eff} \geq 0, \quad \rho^{eff} - p_t^{eff} \geq 0.$

Figure 4 shows that all energy bounds are fulfilled which assure the presence of standard matter in strange star models. The consistency of these bounds also indicates that our proposed $f(R, T)$ model is physically acceptable for all chosen values of the model parameter.

4.3 Compactness and Surface Redshift

The ratio between mass and radius of a stellar object is known as compactness factor. Using the expressions of Heintzmann constants given in (27)-(29), the mass of our stellar system is evaluated as

$$m(r) = \frac{3\mathcal{M} \left[1 + \frac{3\mathcal{R} - 8\mathcal{M} \sqrt{\frac{3(\mathcal{R} - \mathcal{M})}{3\mathcal{R} - 7\mathcal{M}}}}{\mathcal{R} \sqrt{1 + \frac{4\mathcal{M}r^2}{\mathcal{R}^2(3\mathcal{R} - 7\mathcal{M})}}} \right] r^3}{4\mathcal{R}^2 [\mathcal{M} (\frac{r^2}{\mathcal{R}^2} - 7) + 3\mathcal{R}]}. \quad (33)$$

This clearly indicates that the mass function completely depends upon the mass and radius of the strange stars. Equation (33) also states that the mass function becomes zero at the center of star, i.e., at $r = 0$ and shows regular

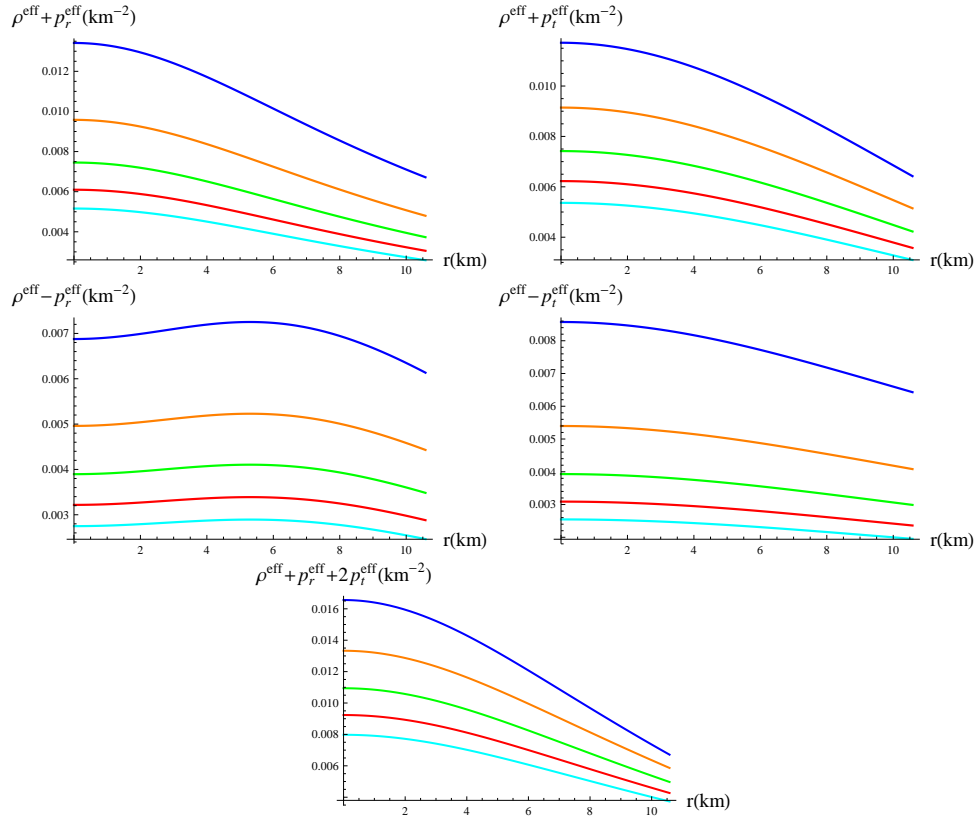


Figure 4: Energy bounds for LMC X-4 with $\sigma = 0$ (blue), $\sigma = 0.2$ (orange), $\sigma = 0.4$ (green), $\sigma = 0.6$ (red) and $\sigma = 0.8$ (cyan).

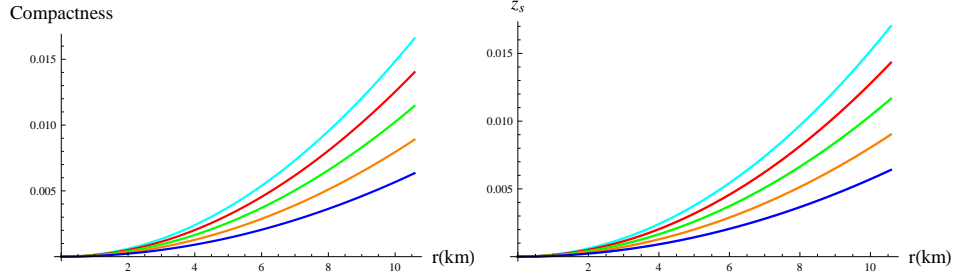


Figure 5: Variation of compactness parameter and surface redshift for LMC X-4 with $\sigma = 0$ (blue), $\sigma = 0.2$ (orange), $\sigma = 0.4$ (green), $\sigma = 0.6$ (red) and $\sigma = 0.8$ (cyan).

behavior within the interior geometry of stellar structure. The compactness factor is defined by

$$u = \frac{m(r)}{r} = \frac{3\mathcal{M}r^2 \left[1 + \frac{3\mathcal{R} - 8\mathcal{M}\sqrt{\frac{3(\mathcal{R}-\mathcal{M})}{3\mathcal{R}-7\mathcal{M}}}}{\mathcal{R}\sqrt{1 + \frac{4\mathcal{M}r^2}{\mathcal{R}^2(3\mathcal{R}-7\mathcal{M})}}} \right]}{4\mathcal{R}^2 \left[\mathcal{M} \left(\frac{r^2}{\mathcal{R}^2} - 7 \right) + 3\mathcal{R} \right]}.$$

The gravitational redshift (z_s) acts as a crucial parameter to interpret the smooth relation between particles in the celestial object and its EoS. In the framework of compactness parameter, the gravitational redshift is expressed in the following form

$$z_s = \frac{1}{\sqrt{1 - \frac{3\mathcal{M}r^2 \left[1 + \frac{3\mathcal{R} - 8\mathcal{M}\sqrt{\frac{3(\mathcal{R}-\mathcal{M})}{3\mathcal{R}-7\mathcal{M}}}}{\mathcal{R}\sqrt{1 + \frac{4\mathcal{M}r^2}{\mathcal{R}^2(3\mathcal{R}-7\mathcal{M})}}} \right]}{2[\mathcal{M}(r^2 - 7\mathcal{R}^2) + 3\mathcal{R}^3]}}} - 1.$$

Substituting the expression of \mathcal{M} and the values of radii, the behavior of compactness as well as redshift parameters is obtained in Figure 5 for different values of σ . These plots manifest that the required Buchdahl condition ($\frac{\mathcal{M}}{\mathcal{R}} < \frac{4}{9}$) [63] is satisfied for compactness factor and the values of redshift parameter are also in the desired range for anisotropic strange star, i.e., $z_s \leq 5.211$ [64].

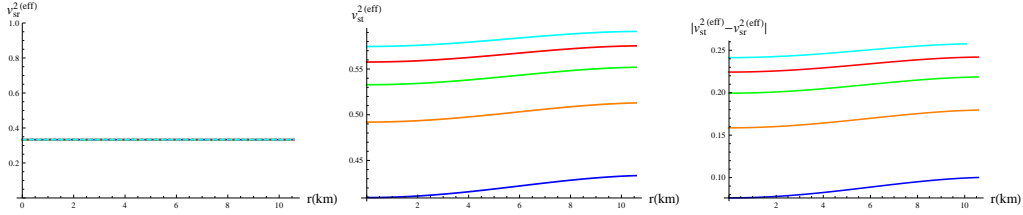


Figure 6: Analysis of stable structure for LMC X-4 with $\sigma = 0$ (blue), $\sigma = 0.2$ (orange), $\sigma = 0.4$ (green), $\sigma = 0.6$ (red) and $\sigma = 0.8$ (cyan).

4.4 Stability Analysis of Stellar Models

The consistency of any physical system can be examined through the stability of that system against external oscillations. The stellar systems with stable structures are considered to be more realistic in astrophysics. In order to investigate the stability of our strange stars candidates, we check the causality condition and the role of adiabatic index. In causality condition for anisotropic fluid, the square of radial (v_{sr}^2) as well as transverse (v_{st}^2) speed of sounds should lie in the range $[0, 1]$ for a physically stable stellar object [11]. Similarly, for a potentially stable system based on Herrera's cracking concept, the difference of radial and transverse sound speeds should possess the same sign everywhere in the matter configuration, i.e., there should be no cracking [11]. Thus the causality as well as Herrera's cracking concept demand that $0 \leq v_{sr}^2 \leq 1$, $0 \leq v_{st}^2 \leq 1$ and $0 \leq |v_{st}^2 - v_{sr}^2| \leq 1$. Here, the square sound speeds are expressed as

$$v_{sr}^{2(eff)} = \frac{dp_r^{eff}}{d\rho^{eff}}, \quad v_{st}^{2(eff)} = \frac{dp_t^{eff}}{d\rho^{eff}}.$$

Figure 6 indicates that LMC X-4 star model has stable structure with both causality and Herrera's cracking concept for the specific values of σ and bag constant.

The validity of any EoS associated with the respective energy density is given by the adiabatic index (Γ). This has gained much attention to explain the stability of both relativistic and non-relativistic stellar bodies. Following the work of Chandrasekhar [65], researchers [66, 67] analyzed the dynamical stability of compact objects against infinitesimal radial adiabatic perturbation. It is proposed that for any dynamically stable celestial object, the adiabatic index should be larger than $\frac{4}{3}$ [66]. For anisotropic matter

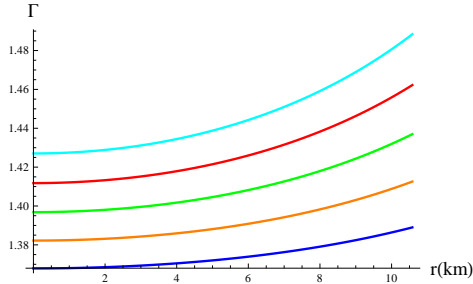


Figure 7: Role of adiabatic index versus r for LMC X-4 with $\sigma = 0$ (blue), $\sigma = 0.2$ (orange), $\sigma = 0.4$ (green), $\sigma = 0.6$ (red) and $\sigma = 0.8$ (cyan).

distribution, the mathematical form of adiabatic index is described as

$$\Gamma = \frac{\rho^{eff} + p_r^{eff}}{p_r^{eff}} \left(\frac{dp_r^{eff}}{d\rho^{eff}} \right).$$

The graphical description of Γ is presented in Figure 7 for different values of σ . This demonstrates that our proposed strange stars exhibit dynamically stable structure for the considered choices of model parameter σ and \mathfrak{B} as the value of $\Gamma > \frac{4}{3}$ throughout the system. Thus, the anisotropic stellar candidates show consistent behavior corresponding to Heintzmann solution in $f(R, T)$ gravity.

5 Final Remarks

This paper is devoted to discuss the influence of MIT bag constant on the physical features of 10 anisotropic strange star candidates in $f(R, T)$ gravity. We have employed the constraints on the metric functions proposed by Heintzmann in which the arbitrary constants (\mathcal{A} , a , c) are determined by a linear relation between both metrics of stellar objects. Using the observed values of masses of considered stars in modified TOV equation, we have evaluated the values of radii, compactness parameter and gravitational redshift for $\mathfrak{B} = 64 \text{MeV}/f\text{m}^3$ (Table 1) which are very close to the values obtained in literature corresponding to the different choices of bag constant [48, 49].

We have obtained the central values of effective matter variables (energy density and radial pressure) for proposed strange star models through graphical analysis and showed their values for $\sigma = 0.8$ (Table 3). We have

presented the diagrammatic interpretation of only LMC X-4 star model for different values of σ . It is found that all the physical quantities indicate positive, regular and finite behavior inside the strange stars that reduce towards the surface of stellar models. For $\mathfrak{B} = 64\text{MeV}/fm^3$, the vanishing condition of the radial pressure is satisfied at $r = \mathcal{R}$ for $\sigma = 0.8$ and the behavior of anisotropic factor is also found to be varying from negative to positive values with increasing values of σ .

From the graphical interpretation of mass-radius relation of strange star, it is obtained that with the larger values of model parameter, the stellar system turns into a more massive and less dense compact object. It is found that all energy bounds are fulfilled for considered stellar models which guarantee the existence of ordinary matter as well as the consistency of our $f(R, T)$ model. The maximum values of the compactness and surface redshift are according to the observational bounds. It is revealed that the stability constraints are satisfied as the inequalities $0 \leq v_{sr}^{2(eff)} \leq 1$, $0 \leq v_{st}^{2(eff)} \leq 1$ and $0 \leq |v_{st}^{2(eff)} - v_{sr}^{2(eff)}| \leq 1$ hold for LMC X-4 star which signifies the existence of potentially stable constitution of quark stars. We have also checked the stability in terms of adiabatic index and observed that $\Gamma > \frac{4}{3}$ which indicates the stability against an infinitesimal radial adiabatic perturbation.

It is observed that the matter-curvature coupling in $f(R, T)$ gravity may provide the more suitable results for ultra-dense compact objects than GR [48]. In this work, we have noticed that strange stars depict regular as well as stable behavior in the framework of Heintzmann solution for MIT bag model EoS and satisfy all the required physical constraints when $\mathfrak{B} = 64\text{MeV}/fm^3$. In graphical analysis, we have presented the behavior of all physical quantities for $\sigma = 0$ which describes the results of GR under the influence of Heintzmann constants. We conclude that the vanishing condition of radial pressure and positive behavior of anisotropic factor are obtained for $\sigma = 0.8$ rather than $\sigma = 0$. Hence, our considered Heint IIa solution along with the specific value of bag constant manifests more viable structure of strange stars in $f(R, T)$ gravity as compared to GR.

Acknowledgment

One (AW) of us would like to thank the Higher Education Commission, Islamabad, Pakistan for its financial support through the *Indigenous Ph.D. 5000 Fellowship Program Phase-II, Batch-III*.

References

- [1] Bodmer, A.R.: Phys. Rev. D **4**(1971)160.
- [2] Baym, G. and Chin, S.A.: Phys. Lett. B **62**(1976)241.
- [3] Witten, E.: Phys. Rev. D **30**(1984)272.
- [4] Alcock, C., Farhi, E. and Olinto, A.: Astrophys. J. **310**(1986)261.
- [5] Haensel, P., Zdunik, J.L. and Schaeffer, R.: Astron. Astrophys. **160**(1986)121.
- [6] Li, X.D., Dai, Z.G. and Wang, Z.R.: Astron. Astrophys. **303**(1995)L1.
- [7] Drago, A., Tambini, U. and Hjorth-Jensen, M.: Phys. Lett. B **380**(1996)13.
- [8] Bombaci, I.: Phys. Rev. C **55**(1997)1587.
- [9] Dey, M. et al.: Phys. Lett. B **438**(1998)123.
- [10] Cheng, K.S., Dai, Z.G. and Lu, T.: Int. J. Mod. Phys. D **7**(1998)139.
- [11] Herrera, L.: Phys. Lett. A **165**(1992)206.
- [12] Demorest, P.B. et al.: Nature **467**(2010)1081.
- [13] Kalam, M. et al.: Int. J. Theor. Phys. **52**(2013)3319.
- [14] Rahaman, F. et al.: Eur. Phys. J. C **74**(2014)3126.
- [15] Bhar, P.: Astrophys. Space Sci. **357**(2015)46.
- [16] Murad, M.H.: Astrophys. Space Sci. **361**(2016)20.
- [17] Arbañil, J.D.V. and Malheiro, M.: J. Cosmol. Astropart. Phys. **11**(2016)012.
- [18] Deb, D. et al.: Ann. Phys. **387**(2017)239.
- [19] Capozziello, S.: Int. J. Mod. Phys. D **483**(2002)11; Nojiri, S. and Odintsov, S.D.: Phys. Rev. D **68**(2003)123512; Carroll, S.M. et al.: Phys. Rev. D **70**(2004)043528; Nojiri, S. and Odintsov, S.D.: Phys. Rev. D **74**(2006)086005; Bertolami, O. et al.: Phys. Rev. D **75**(2007)104016.

- [20] Cognola, G. et al.: Phys. Rev. D **73**(2006)084007; Li, B., Barrow, J.D. and Mota, D.F.: Phys. Rev. D **76**(2007)044027; Bamba, K. et al.: Eur. Phys. J. C **67**(2010)295.
- [21] Bengochea, G.R. and Ferraro, R.: Phys. Rev. D **79**(2009)124019; Linder, E.V.: Phys. Rev. D **81**(2010)127301.
- [22] Harko, T. et al.: Phys. Rev. D **84**(2011)024020.
- [23] Haghani, Z. et al.: Phys. Rev. D **88**(2013)044023; Odintsov, S.D. and Sáez-Gómez, D.: Phys. Lett. B **725**(2013)437.
- [24] Sharif, M. and Ikram, A.: Eur. Phys. J. C **76**(2016)640.
- [25] Sharif, M. and Zubair, M.: J. Cosmol. Astropart. Phys. **03**(2012)028.
- [26] Sharif, M. and Zubair, M.: J. Phys. Soc. Jpn. **81**(2012)114005.
- [27] Jamil, M., Momeni, D. and Myrzakulov, R.: Chin. Phys. Lett. **29**(2012)109801.
- [28] Sharif, M. and Zubair, M.: J. Phys. Soc. Jpn. **82**(2013)064001; *ibid.* 014002.
- [29] Shabani, H. and Farhoudi, M.: Phys. Rev. D **88**(2013)044048.
- [30] Sharif, M. and Zubair, M.: Gen. Relativ. Gravit. **46**(2014)1723.
- [31] Shabani, H. and Farhoudi, M.: Phys. Rev. D **90**(2014)044031.
- [32] Moraes, P.H.R.S.: Eur. Phys. J. C **75**(2015)168.
- [33] Momeni, D., Myrzakulov, R. and Güdekli, E.: Int. J. Geom. Meth. Mod. Phys. **12**(2015)1550101.
- [34] Moraes, P.H.R.S.: Int. J. Theor. Phys. **55**(2016)1307.
- [35] Alhamzawi, A. and Alhamzawi, R.: Int. J. Mod. Phys. D **25**(2015)1650020.
- [36] Moraes, P.H.R.S., Arbañil, J.D.V. and Malheiro, M.: J. Cosmol. Astropart. Phys. **06**(2016)005.

- [37] Zubair, M., Abbas, G. and Noureen, I.: *Astrophys. Space Sci.* **361**(2016)8.
- [38] Sharif, M. and Siddiqa, A.: *Eur. Phys. J. Plus* **132**(2017)529.
- [39] Das, A.: *Phys. Rev. D* **95**(2017)124011.
- [40] Yousaf, Z., Bhatti, M.Z. and Ilyas, M.: *Eur. Phys. J. C* **78**(2018)307.
- [41] Sharif, M. and Waseem, A.: *Gen. Relativ. Gravit.* **50**(2018)78.
- [42] Deb, D. et al.: *J. Cosmol. Astropart. Phys.* **03**(2018)044.
- [43] Sharif, M. and Waseem, A.: *Eur. Phys. J. C* **50**(2018)78.
- [44] Sharif, M. and Siddiqa, A.: *Int. J. Mod. Phys. D* **27**(2018)1850065.
- [45] Deb, D. et al.: *Phys. Rev. D* **97**(2018)084026.
- [46] Sharif, M. and Waseem, A.: *Int. J. Mod. Phys. D* **28**(2019)1950033.
- [47] Biswas, S. et al.: *Ann. Phys.* **401**(2019)1.
- [48] Deb, D. et al.: *Mon. Not. R. Astron. Soc.* **485**(2019)5652.
- [49] Maurya, S.K. et al.: *Phys. Rev. D* **100**(2019)044014.
- [50] Das, A. et al.: *Eur. Phys. J. C* **76**(2016)654.
- [51] Sharif, M. and Siddiqa, A.: *Eur. Phys. J. Plus* **133**(2018)226.
- [52] Sharif, M. and Siddiqa, A.: *Ad. High Energy Phys.* **2019**(2019)8702795.
- [53] Heintzmann, H.: *Z. Phys.* **228**(1969)489.
- [54] Estrada, M. and Tello-Ortiz, F.: *Eur. Phys. J. Plus* **133**(2018)453.
- [55] Morales, E. and Tello-Ortiz, F.: *Eur. Phys. J. C* **78**(2018)618.
- [56] Abubekerov, M.K. et al.: *Astron. Rep.* **52**(2008)379.
- [57] Elebert, P. et al.: *Mon. Not. R. Astron. Soc.* **395**(2009)884.
- [58] Özel, F., Güver, T. and Psaltis, D.: *Astrophys. J.* **693**(2009)1775.

- [59] Güver, T. et al.: *Astrophys. J.* **719**(2010)1807.
- [60] Rawls, M. et al.: *Astrophys. J.* **730**(2011)25.
- [61] Freire, P.C.C. et al.: *Mon. Not. R. Astron. Soc.* **412**(2011)2763.
- [62] Chakraborty, S.: *Gen. Relativ. Gravit.* **45**(2013)2039.
- [63] Buchdahl, H.A.: *Phys. Rev.* **116**(1959)1027.
- [64] Ivanov, B.V.: *Phys. Rev. D* **65**(2002)104011.
- [65] Chandrasekhar, S.: *Astrophys. J.* **140**(1964)417.
- [66] Heintzmann, H. and Hillebrandt, W.: *Astron. Astrophys.* **38**(1975)51.
- [67] Hillebrandt, W. and Steinmetz, K.O.: *Astron. Astrophys.* **53**(1976)283;
Bombaci, I.: *Astron. Astrophys.* **305**(1996)871.